Mol Neurobiol
DOI 10.1007/s12035-014-8969-1

G206D Mutation of Presenilin-1 Reduces Pen2 Interaction, Increases Aβ42/Aβ40 Ratio and Elevates ER Ca^{2+} Accumulation

Wei-Ting Chen · Yi-Fang Hsieh · Yan-Jing Huang · Che-Ching Lin · Yen-Tung Lin · Yu-Chao Liu · Cheng-Chang Lien · Irene Han-Juo Cheng

Received: 24 September 2014 / Accepted: 28 October 2014

Abstract Early-onset familial Alzheimer's disease (AD) is most commonly associated with the mutations in presenilin-1 (PS1). PS1 is the catalytic component of the γ-secretase complex, which cleaves amyloid precursor protein to produce amyloid-β (Aβ), the major cause of AD. Presenilin enhancer 2 (Pen2) is critical for activating γ-secretase and exporting PS1 from endoplasmic reticulum (ER). Among all the familial AD-linked PS1 mutations, mutations at the G206 amino acid are the most adjacent position to the Pen2 binding site. Here, we characterized the effect of a familial AD-linked PS1 G206D mutation on the PS1-Pen2 interaction and the accompanied alteration in γ-secretase-dependent and -independent functions. We found that the G206D mutation reduced PS1-Pen2 interaction, but did not abolish γ-secretase formation and PS1 endoproteolysis. For γ-secretase-dependent function, the G206D mutation increased $A\beta_{42}$ production but not Notch cleavage. For γ-secretase-independent function, this mutation disrupted the ER calcium homeostasis but not lysosomal calcium homeostasis and autophagosome maturation. Impaired ER calcium homeostasis may due to the reduced mutant PS1 level in the ER. Although this mutation did not alter the cell survival under stress, both increased $A\beta_{42}$ ratio and disturbed ER calcium regulation could be the mechanisms underlying the pathogenesis of the familial AD-linked PS1 G206D mutation.

Keywords Alzheimer's disease · Presenilin-1 · Presenilin enhancer 2 · G206D mutation · Amyloid beta · Calcium

Electronic supplementary material The online version of this article (doi:10.1007/s12035-014-8969-1) contains supplementary material, which is available to authorized users.

W.-T. Chen
Taiwan International Graduate Program in Molecular Medicine, National Yang-Ming University and Academia Sinica, Taipei, Taiwan

W.-T. Chen · Y.-F. Hsieh · C.-C. Lin · Y.-T. Lin · I. H.-J. Cheng
Institute of Brain Science, National Yang-Ming University, Taipei, Taiwan

W.-T. Chen
Institute of Biochemistry and Molecular Biology, School of Life Science, National Yang-Ming University, Taipei, Taiwan

Y.-J. Huang
Department of Life Sciences and Institute of Genome Sciences, National Yang-Ming University, Taipei, Taiwan

Y.-C. Liu · C.-C. Lien
Institute of Neuroscience, National Yang-Ming University, Taipei, Taiwan

C.-C. Lien · I. H.-J. Cheng
Brain Research Center, National Yang-Ming University, Taipei, Taiwan

I. H.-J. Cheng
Infection and Immunity Research Center, National Yang-Ming University, Taipei, Taiwan

I. H.-J. Cheng
Immunology Center, Taipei Veterans General Hospital, Taipei, Taiwan

I. H.-J. Cheng (✉)
Institute of Brain Science, School of Medicine, National Yang-Ming University, No. 155, Sec. 2, Linong Street, Taipei 112, Taiwan
e-mail: hjcheng@ym.edu.tw

Published online: 15 November 2014

Introduction

Alzheimer's Disease and Amyloid-Beta (Aβ) Peptide

Alzheimer's disease (AD) is the most common form of age-dependent dementia [1]. One of the pathological hallmarks of AD is amyloid plaque, which mainly consists of aggregated amyloid-β (Aβ), a 38–49-amino acid peptide. Aβ is produced through the sequential cleavage of amyloid precursor protein (APP) by β- and γ-secretases [2]. Among the secreted Aβs, $Aβ_{40}$ is the predominant species, but $Aβ_{42}$ has higher tendency to form neurotoxic aggregates. These Aβ aggregates are believed to be the initiator of AD [3, 4].

Presenilin and γ-Secretase

γ-Secretase complex consists of presenilin (PS), nicastrin (Nct), anterior pharynx-defective 1 (Aph1), and presenilin enhancer 2 (Pen2) [5, 6]. PS is the catalytic component of γ-secretase that cleaves APP and other proteins such as Notch [7, 8]. Vertebrates have two presenilin genes, named *PSEN1* that encodes presenilin 1 (PS1) and *PSEN2* that encodes presenilin 2 (PS2). PS1-associated γ-secretase displays higher activity than PS2 [9]. PS1 resides at the membrane of endoplasmic reticulum (ER) and endosomal system [10–12]. Binding of Pen2 regulates PS1 export from ER to endosomal system and other compartments [13]. The residue in PS1 essential for the Pen2 binding is the polar amino acid N204 [14–16]. Pen2 binding induces PS1 endoproteolysis to generate the active form of γ-secretase [6]. In the process of PS1 endoproteolysis, the 50 kDa PS1 holoprotein cleaves itself to produce a 30 kDa N-terminal fragment (PS1-NTF) and a 20 kDa C-terminal fragment (PS1-CTF), both of which are essential to the catalytic site.

γ-Secretase has at least two different enzymatic activities, ε- and γ-cleavages [17–19]. Following the β-secretase cleavage of APP to produce C99, ε-cleavage activity acts on C99 to produce long Aβs ($Aβ_{48}$ and $Aβ_{49}$). These long Aβs are further processed by γ-cleavage activity to release a mixture of Aβ species [17]. Apart from APP, γ-secretase cleaves many other transmembrane proteins such as Notch. ε-Cleavage on Notch yields notch intracellular domain (NICD) [19, 20], which modifies gene expression in many cell types. The PS1 knockout mice lead to an embryonic lethal phenotype similar to the mice lacking Notch [21, 22].

PS1 Function Independent of γ-Secretase Activity

Independent of γ-secretase activity, PS1 has diverse biological roles [23] in the regulation of intracellular calcium homeostasis [24] and the proteolysis through autophagy-lysosome system [25]. Deficiency of PS leads to ER Ca^{2+} accumulation and excess intracellular Ca^{2+} signals [24, 26–29], which is important for regulating neurotransmission and synaptic plasticity [30]. The disturbed ER Ca^{2+} homoeostasis by PS1 mutations is linked to the early presynaptic deficits in AD [30–33].

Deficiency of PS also leads to autophagosome accumulation [25, 34], which might be resulted from the failure of lysosomal acidification [25] or lysosomal Ca^{2+} release [35, 36]. Lysosomal fusion with autophagosome is necessary for efficient proteolysis and neuron survival. However, the mechanism on whether PS1 directly or indirectly regulates lysosomal Ca^{2+} homeostasis remains controversial [37–39]. In addition, PS1 regulates many signaling pathways essential for cell survival. Several PS1 mutants fail to activate pro-survival signaling and reduce cell survival under stress conditions [40].

Discovery of the PS1 G206D Mutation

Early onset (<65 years of age) familial AD (FAD) usually associates with three genes: *APP*, *PSEN1*, and *PSEN2* [41]. Previously, we reported a Taiwanese family of early-onset AD characterized by a rapid deterioration course, appearance of cotton wool-like plaque, and seizure, with a G→A substitution in the position 617 at exon 7 of *PSEN1* gene causing a glycine to aspartate acid substitution of PS1 protein at amino acid 206 (G206D) [42]. This G206D mutation has also been reported in the other family [43], but the detailed pathogenic mechanism is still unclear. Among all the FAD PS1 mutations, the G206D mutation is the one most adjacent to the Pen2 binding site (N204). In this study, we explore the effects of the G206D mutation on γ-secretase-dependent and -independent PS1 functions. This study would provide the genetic evidence for the contribution of Pen2 in the pathogenesis of AD.

Methods

Cell Culture Wild-type, PS1-null, and PS1/2-null mouse embryonic fibroblast (MEF) [9] were maintained in Dulbecco's modified Eagle's medium (DMEM, 12100–046, Gibco, CA, USA). Human neuroblastoma SH-SY5Y-APP (stably overexpressing APP695) cells were maintained in Minimum Essential Medium (MEM, 41500–034, Gibco, CA, USA), F-12 nutrient mixture (21700–075, Gibco, CA, USA), and 400 μg/ml puromycin. Human embryonic kidney (HEK293T) cells and COS7 cells were maintained in DMEM. All culture media were supplemented with 10 % fetal bovine serum (FBS, SH3007, HyClone, UT, USA), 1 % L-glutamine (GLL01, Caisson laboratory, UT, USA), and 100 μg/ml penicillin-streptomycin (PSL01, Caisson laboratory, UT, USA), and maintained at 37 °C in 5 % CO_2. Cells were transiently transfected with either PS1 variants or control

vector using Lipofectamine 2000 (11668–019, Invitrogen, CA, USA) or Turbofect (R0531, Thermo Scientific, MA, USA; only for Fig. 5).

cDNA Constructs The constructs we applied include the HA-tagged human APH1 cDNA, or FLAG-tagged human PEN2 cDNA in pcDNA3.1/Zeo(+) plasmid [44], the wild-type human PS1 cDNA in pcDNA3.1/Zeo(+) plasmid [45], the DsRed-GFP-LC3 cDNA in pDsRed-Monomer-C1 plasmid [46], the NotchΔmyc or V/LΔmyc constructs [47], the EGFP-Sec61β or EGFP-Rab5 constructs [48], and the pEGFP-C1 construct (GenBank Accession no. U55763, Catalog no. 6084-1, Clontech, CA, USA). The G206D mutation in PS1 cDNA was introduced by standard site-directed mutagenesis (QuikChange II Site-Directed Mutagenesis Kit, STRATAGENE, CA, USA). For the EGFP-PS1 construct, the PS1 cDNA was clipped out by *KpnI* and *Xba1* restriction enzymes, acting at 5′ end and 3′ end of the human PS1 cDNA containing pcDNA5/TO plasmid [45], respectively. The PS1 cDNA variants were then inserted into the *KpnI-Xba1* site of pEGFP-C1. The GFP-PS1 variants are endoproteolytically processed [Electronic Supplementary Material (ESM) Fig. 1], indicating the generation of active form of γ-secretase, but full functionality has not been completely tested.

Immunoprecipitation (IP) Analysis Twenty-eight hours after transfection, HEK293T cells were directly extracted with IP buffer (5 mM HEPES, 1 % CHAPSO and the complete protease inhibitor cocktail tablet, Roche, CA, USA) for 1 h on ice. After centrifugation (3,000×*g*, 4 °C, 10 min), 100 μg of total protein from supernatant was pre-cleared by protein G beads (LSKMAGXX, Millipore, MA, USA). For IP-Aph1, lysates were incubated with anti-PS1 loop antibodies (1:1000, MAB5232, Millipore, MA, USA). For IP-Pen2, lysates were incubated with anti-PS1 NTF antibodies (1:1000, MAB1563, Millipore, MA, USA). The IP reactions were performed at 4 °C overnight with gentle rotation and then precipitated by protein G beads at room temperature for 1 h. After washing three times with washing buffer (1 % Tritone X-100 and 3 % BSA in PBS), proteins were eluted with 1X SDS sample buffer at 37 °C for 20 min. Western blotting result was quantified and the interactions were calculated as: (IP-APH1/total-APH1) or (IP-PEN2/total-PEN2)/(IP-PS1/total-PS1).

Gel Electrophoresis and Western Blotting Analysis Proteins were separated by 10 % Tris-Glycine SDS-polyacrylamide gel electrophoresis (PAGE), except the proteins from IP were separated by 10 and 15 % Tricine-SDS PAGE, and transferred to nitrocellulose membranes. Membranes were probed by primary antibodies: mouse anti-APP (6E10, NE1003, Millipore, MA, USA), mouse anti-PS1 loop (MAB5232, Millipore, MA, USA), rat anti-PS1NTF (MAB1563, Millipore, MA, USA), mouse anti-myc (9E10, 05–419, Millipore, MA, USA), mouse anti-Flag (F3165, Sigma, MO, USA), mouse anti-actin (MAB1501, Millipore, MA, USA), and mouse anti-GAPDH (GTX100118, Genetex, CA, USA). Membranes were washed and probed with HRP-conjugated affinity-purified secondary antibodies: goat anti-mouse IgG, goat anti-rat IgG, and goat anti-rabbit IgG (12–349, AP136P, AP132P, Millipore, MA, USA). Protein signals were developed with chemiluminescent substrate ECL detection system (WBKLS0500, Millipore, MA, USA) and quantified by luminescence imaging system (LAS-4000, Fujifilm, Japan).

Cellular Organelle Fractionation The ER isolation kit (ER0100, Sigma, MO, USA) was applied. Briefly, HEK293T cells transfected with $PS1^{wt}$ or $PS1^{G206D}$ were mildly broken by pestle for 15 strokes. After differential centrifugation, the ER-enriched fraction was precipitated by 7 mM $CaCl_2$ in the post mitochondria fraction. The ER-enriched fractions were either directly visualized by Western blotting or further separated by 15–30 % Optiprep™ (ER0100, Sigma, MO, USA) density gradient (0.5 ml of 30 %, 1 ml of 25 %, 1 ml of 20 % with samples, 1.5 ml of 15 %). After ultracentrifugation (rotor SW55 Ti, 3 h at 4 °C, 35,000 rpm, 150,000×*g*), eight fractions were collected from the top to the bottom and analyzed by Western blotting. Result is quantified and calculated as: PS1 in ER-enriched fraction/PS1 in total lysate/ER marker.

Immunocytochemistry COS7 cells were co-transfected PS1 with either GFP-Sec61β or GFP-Rab5. Cells were fixed in 4 % paraformaldehyde in PBS at 4 °C overnight and then blocked and permeabilized by 10 % FBS containing 0.3 % Triton X-100 for 1 h at room temperature. Fixed cells were incubated with anti-PS1-loop antibody (MAB5232, Millipore, MA, USA) overnight at 4 °C and next with Cy3-conjugated goat anti-mouse IgG (115-165-003, Jackson ImmunoResearch, PA, USA) for 2 h at room temperature. Images were captured by confocal microscope (FV1000, Olympus, Japan). Co-localization was analyzed by image analysis software (MetaMorph Premier, Molecular Devices, CA, USA).

Enzyme-Linked Immunosorbent Assay (ELISA) The levels of $Aβ_{total}$ and $Aβ_{42}$ were measured by human amyloid-β (1–42) and amyloid-β (1–*x*) assay kit (IBL). Forty-eight hours after transfection, conditioned media were incubated with capture antibody overnight and followed by the HRP conjugated anti-human Aβ (11–28) antibody for 1 h at 4 °C. Color was developed by tetramethylbenzidine chromogen and read at 450 nm by microplate reader (Sunrise, TECAN, Switzerland).

Fura-2-AM Ca^{2+} Imaging Experiments Intracellular Ca^{2+} concentration was measured by a dual wavelength ratiometric method [49]. Fura-2-AM stock was dissolved in pluronic F-127 (20 % solution in DMSO, P-3000MP, Life technologies,

CA, USA). MEFs were cultured on poly-D-lysine-coated coverslips and transfected with GFP-PS1^{wt} or GFP-PS1^{G206D}. The transfected cells were identified by GFP imaging. Forty-eight hours after transfection, cells were stained with 5 μM Fura-2-AM (F1221, Invitrogen, CA, USA) in HEPES buffer (140 mM NaCl, 5 mM KCl, 1 mM $MgCl_2$, and 10 mM HEPES, pH 7.3) containing 2 mM $CaCl_2$ for 1 h at room temperature. Immediately before imaging, cells were shifted to Ca^{2+} free HEPES buffer containing 100 μM EGTA. Fura-2-AM signals were excited by polychrome V monochromator (TILL Photonic, Germany) at 340- and 380-nm wavelengths with 200-ms exposure time. Images were collected every 5 s using an EM-CCD camera (QuantEM 512SC, Photometrics, AZ, USA) mounted on an upright microscope (BX51WI, Olympus, Japan). Ionomycin (Asc-370, Ascent, UK), thapsigargin (Asc-286, Ascent, UK), and gly-Phe-β-naphtylamide (sc-252858, Santa cruz, TX, USA) were applied to induce Ca^{2+} signals. Region of interest was defined by the margin of the transfected cell. After background subtraction, fluorescence intensity was quantified by MetaFluor Fluorescence Ratio Imaging Software (Molecular Device, CA, USA).

The absolute value of cytosolic Ca^{2+} concentration ($[Ca^{2+}]_i$) was determined by the equation [49]:

$$\left[Ca^{2+}\right] = K_d \frac{[R-R_{min}]}{[R_{max}-R]} \frac{Sf380}{Sb380}$$

where the Fura-2 affinity (K_d) to Ca^{2+} is 140 nM, R is the experimentally determined 340/380 ratio, R_{max} is the 340/380 ratio of Ca^{2+}-saturated Fura-2 (addition of 20 mM Ca^{2+} and 10 μM ionomycin), R_{min} is the 340/380 ratio of Ca^{2+}-free Fura-2 (addition of 10 mM EGTA), and S_{f380}/S_{b380} is the ratio of fluorescence intensity of Ca^{2+}-free and Ca^{2+}-bound form of Fura-2 at 380 nm.

Autophagy Assay The autophagosome accumulation or lysosomal dysfunction is measured by the ratio of GFP to DsRed fluorescence intensity in DsRed-GFP-LC3 reporter transfected cells [50]. Twenty-four hours after transfection, cells were collected and fixed by 1 % PFA. Fluorescence intensity of GFP or DsRed was measured by flow cytometry and analyzed by Cell Quest software. Quantified result is shown as the normalization of the ratio of GFP to DsRed to that of the wild-type control.

Apo-BrdU-Red^{TM} In Situ BrdU (TUNEL) Labeling Assay DNA fragmentation was labeled using Apo-BrdU-Red^{TM} in situ DNA Fragmentation assay kit (Biovision, CA, USA). Twenty-four hours after transfection, HEK293T cells expressing GFP or GFP-PS1 variants were treated with 1,500 μM H_2O_2 for 24 h and then fixed with 4 % paraformaldehyde. Fixed cells were incubated in DNA labeling solution for 1 h at 37 °C, stopped the reaction with rinse buffer, and then incubated with anti-BrdU-Red antibodies for 30 min at room temperature. Labeled signals were analyzed by flow cytometry within 3 h after staining.

Propidium Iodide Staining for Cell Cycle Analysis Propidium iodide (PI, Sigma, MO, USA) was used to stain DNA content [51]. Twenty-four hours after transfection, HEK293T cells were treated with 1500 μM H_2O_2 for 24 h and fixed by 70 % ice-cold ethanol. Fixed cells were resuspended in 0.5 ml PBS and incubated in 0.5 ml DNA extraction buffer (192 mM $NaHPO_4$, 0.004 % Triton X-100, pH 7.8) for 5 min at room temperature and centrifuged for 5 min. Cell pellets were re-suspended in 1 ml DNA staining solution (20 μg/ml propidium iodide, 200 μg/ml DNase-free RNase) for 30 min in the dark at room temperature and analyzed by flow cytometry within 3 h after staining.

Flow Cytometry Samples were analyzed by flow cytometry (FACSCalibur, BD, NJ, USA) using Cell Quest software. Fluorescence was excited by 488-nm argon-laser and detected through 530/30 nm (FL1 channel) and 585/42 nm (FL2 channel) band pass filter. Non-transfected cells without staining were used to define the threshold and to amplify adjustment. Transfected cells were used to compensate fluorescence crosstalk. For TUNEL assay, DNA fragmentation was labeled with BrdUTP, probed by anti-BrdU antibody conjugating with Cy3 (Em, 576 nm), and detected by FL2-H channel. For PI staining, after filtering out single cells by area-width plot, the DNA content of single cells was detected by FL2-A channel. Cell cycle was analyzed by FlowJo version 7.6.1 under appropriate constraints employing Dean-Jett-Fox model [52].

Result

The G206D Mutation Reduces the PS1-Pen2 Interaction But Does Not Abolish γ-Secretase Activation

The G206D mutation is adjacent to the amino acids N204 crucial for PS1 interacting with Pen2, which is a required step for γ-secretase activation [6, 14, 15]. To examine γ-secretase formation, we co-transfected Pen2 or Aph1 with PS1^{wt} or PS1^{G206D} into HEK293T cells and analyzed their interaction by co-immunoprecipitation (Fig. 1a). The levels of Aph1 co-immunoprecipitated with PS1^{wt} (set as 1) or PS1^{G206D} (0.936 ±0.167) had no significant difference, but the levels of Pen2 co-immunoprecipitated with PS1^{G206D} (0.331±0.135) were significantly lower than that with PS1^{wt} (set as 1) (Fig. 1b). This result indicates that the G206D mutation partially

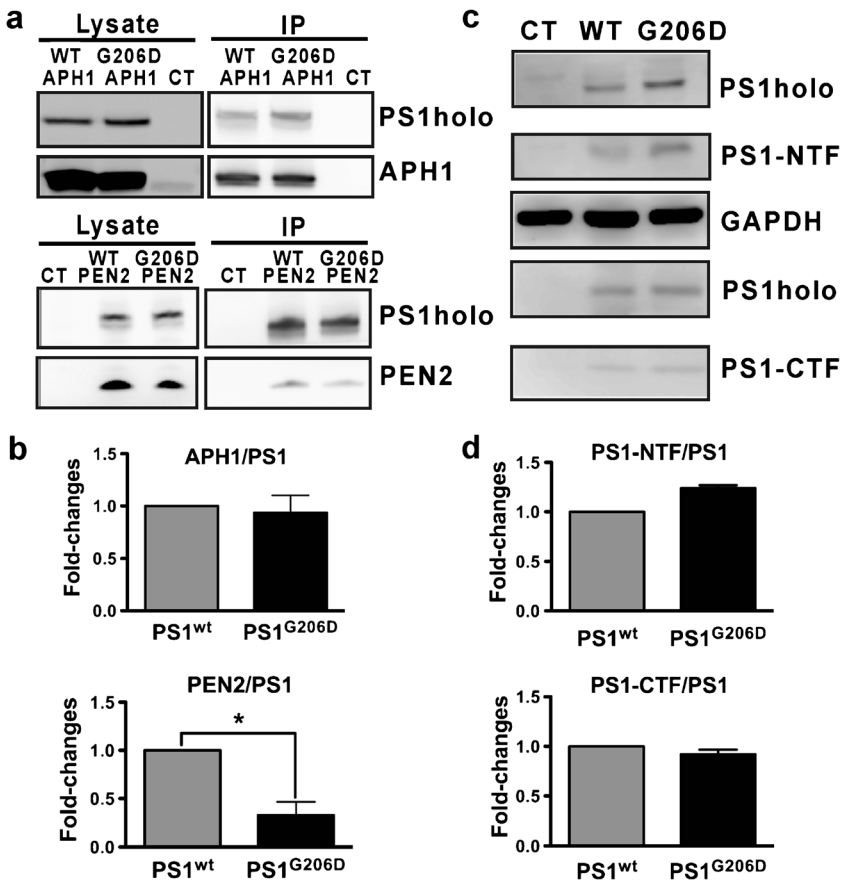

Fig. 1 The PS1 G206D mutation reduced PS1-Pen2 interaction but not PS1 endoproteolysis. **a** Co-immunoprecipitation was used to determine the formation of γ-secretase complex. Aph1 was co-immunoprecipitated with PS1-CTF specific antibody, while Pen2 was co-immunoprecipitated with PS1-NTF specific antibody. **b** PS1-Aph1 and PS1-Pen2 interactions were analyzed by the normalization of the IP-lysate to the total-lysate: (IP-Aph1/total-Aph1) or (IP-Pen2/total-Pen2) / (IP-PS1/total-PS1). The level of co-immunoprecipitated Aph1 (*upper*) had no difference between $PS1^{wt}$- and $PS1^{G206D}$-expressing cells, but the level of co-immunoprecipitated Pen2 (*lower*) was significantly lower in $PS1^{G206D}$-expressing cells than that in $PS1^{wt}$-expressing cells. **c** Representative Western blotting images show the levels of PS1 holoprotein, PS1-NTF, and PS1-CTF at 36 h after transfection of $PS1^{wt}$, $PS1^{G206D}$, or control plasmid (CT) into PS1-null MEFs. **d** The levels of PS1-NTF (*upper*) or PS1-CTF (*lower*) over PS1 holoprotein were not significantly different between $PS1^{wt}$- and $PS1^{G206D}$-expressing cells. Data are represented as the mean ±SD (n=3 independent transfection, *p<0.05 by t test)

reduces PS1-Pen2 interaction but does not abolish the γ-secretase formation.

PS1 endoproteolysis is required for the γ-secretase activation. To test PS1 endoproteolysis, we measured the levels of PS1 holoprotein and endoproteolytic fragments (PS1-CTF and PS1-NTF) in PS-null MEF transfected with $PS1^{wt}$ or $PS1^{G206D}$ (Fig. 1c). The proportion of endoproteolytic fragments over total PS1 in $PS1^{wt}$ (set as 1) or $PS1^{G206D}$ (CTF, 0.921±0.046; NTF, 1.24±0.028) had no significant difference, suggesting normal endoproteolytic activity of γ-secretase (Fig. 1d). Thus, the G206D mutation did not abolish the PS1 endoproteolysis.

The G206D Mutation Increases the Production of Aβ42 But Not NICD

PS1 mutations could alter the γ-secretase activity toward APP and Notch, producing more $A\beta_{42}$ but less NICD [53, 54]. Thus, we measured the levels of Aβ and NICD in $PS1^{wt}$- or $PS1^{G206D}$-expressing cells.

To examine the effect of the G206D mutation on levels of $A\beta_{42}$ and $A\beta_{total}$, SHSY-5Y cells stably expressing APP (SHSY-5Y-APP) were transfected with $PS1^{wt}$ or $PS1^{G206D}$. Secreted Aβ level in the culture media was measured by ELISA, and expression levels of $PS1^{wt}$ or $PS1^{G206D}$ were monitored by Western blotting. Although there was no significant difference in $A\beta_{total}$ level among all groups, the $A\beta_{42}$ level of $PS1^{G206D}$-expressing cells (2.054±0.784 ng/ml) was significantly higher than that of the untransfected control (0.529±0.205 ng/ml) (Fig. 2a, b). The $A\beta_{42}/A\beta_{total}$ ratio in $PS1^{G206D}$-expressing cells (2.13±0.347-fold higher than control) was significantly higher than that in $PS1^{wt}$-expressing cells (1.541±0.3-fold higher than control) (Fig. 2c), suggesting that the G206D mutation promotes the production of $A\beta_{42}$.

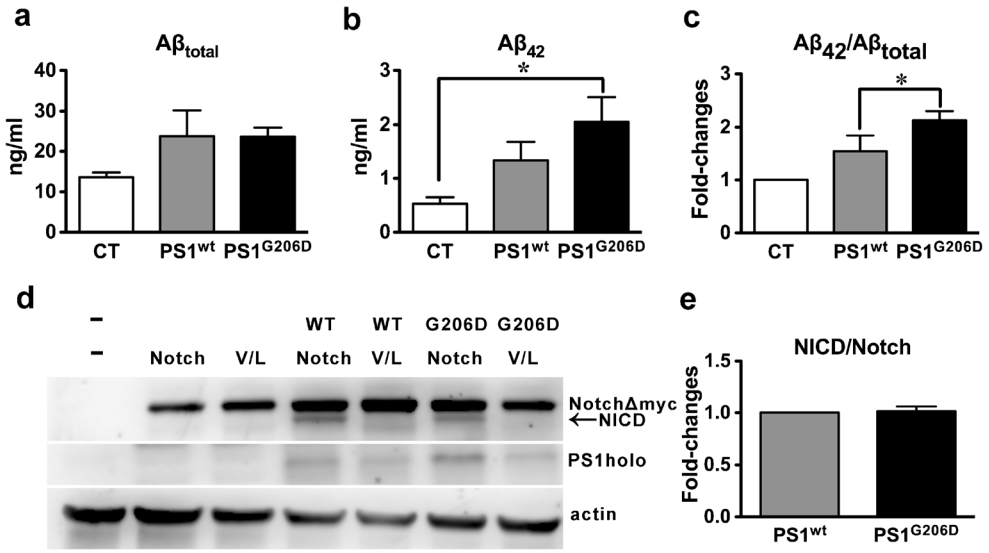

Fig. 2 The PS1 G206D mutation increased $A\beta_{42}$ ratio but not NICD levels. **a**–**c** To measure the Aβ production, SHSY-5Y-APP culture media were collected at 36 h after transfection of $PS1^{wt}$ or $PS1^{G206D}$. $A\beta_{42}$ and $A\beta_{total}$ levels in these media were measured by ELISA. **a** The concentration of $A\beta_{total}$ was not significantly different among these 3 groups. **b** The concentration of $A\beta_{42}$ was significantly higher in $PS1^{G206D}$-expressing cells than the mock-transfected control (CT). **c** The ratio of $A\beta_{42}/A\beta_{total}$ was significantly higher in $PS1^{G206D}$-expressing cells. The fold change of $A\beta_{42}/A\beta_{total}$ ratio in CT was set as 1. **d**, **e** To measure the NICD production, NotchΔmyc or V/LΔmyc was co-transfected with PS1 variants into PS1-null MEF. **d** Representative Western blotting images show the levels of NICD and PS1 holoprotein. V/LΔmyc construct that could not be cleaved by γ-secretase was used as a negative control. **e** The ratio of NICD to Notch (NotchΔmyc) was normalized to mock-transfected control (CT, NotchΔmyc expression only) group (*set as 1*). There was no difference between the two groups. Data are presented as the mean ±SD (n=3 independent transfection, *p<0.05. by ANOVA)

To explore whether the G206D mutation alters γ-secretase activity toward Notch, truncated Notch sequence fused with 6x myc tags (NotchΔmyc) was used as a reporter for NICD production. The same construct containing a V1742L mutation (V/LΔmyc) to disrupt the γ-secretase cleavage was used as a negative control [47, 55]. The Notch reporters were co-transfected with $PS1^{wt}$ or $PS1^{G206D}$ into PS1-null MEF cell, and the Notch and NICD levels were measured by Western blotting (Fig. 2d). There was no difference in NICD/Notch ratio between $PS1^{wt}$- (set as 1) and $PS1^{G206D}$-expressing cells (1.014±0.047) (Fig. 2e). Thus, γ-secretase activity toward Notch is similar between $PS1^{G206D}$ and $PS1^{wt}$. Together, our result shows that the G206D mutation increases the ratio of $A\beta_{42}$ to $A\beta_{total}$ without affecting NICD levels.

The G206D Mutation Disrupts the ER Ca^{2+} Homeostasis

Apart from the role in γ-secretase, PS1 also regulates the homeostasis of Ca^{2+} in ER [24, 26, 27]. To examine ER Ca^{2+} level, we depleted ER Ca^{2+} storage in MEF by ionomycin (IO) or thapsigargin (TG) (Fig. 3a). IO is an ionophore that induces formation of Ca^{2+}-permeable pores. Because ER Ca^{2+} is the major intracellular Ca^{2+} pool, IO-induced signal is frequently used to implicate the calcium storage of ER [24, 56, 57]. TG is a specific inhibitor of the smooth ER Ca^{2+}-ATPase (SERCA) pump, thereby blocking Ca^{2+} pumped into ER while allowing the passive Ca^{2+} leak. Application of 5 μM IO or 1 μM TG in the absence of extracellular Ca^{2+} evoked larger areas under curves in the PS-null MEF compared with the control MEF (Fig. 3b). The average area under curve induced by IO- or TG-sensitive Ca^{2+} pools in PS-null MEF (IO, 82.97±13.65; TG, 133.3±17.86 μM×s) was significantly larger than the control MEF (IO, 33.51±8.45; TG, 42.04±6.2 μM×s) (Fig. 3c), which is consistent with previous reports on the essential role of PS1 in preventing ER Ca^{2+} over-accumulation [24, 26, 27].

To examine whether $PS1^{G206D}$ impairs ER Ca^{2+} homeostasis, we transfected GFP, GFP-$PS1^{wt}$, or GFP-$PS1^{G206D}$ into PS-null MEF. The IO or TG-evoked Ca^{2+} signals were larger in GFP-$PS1^{G206D}$-expressing cells (IO, 109.22±22.15; TG, 55.46±6.87 μM×s) compared with GFP-$PS1^{wt}$-expressing cells (IO, 45.75±9.97; TG, 27.78±2.97 μM×s) (Fig. 3d, f). Our result suggests that $PS1^{G206D}$ losses the ability to regulate ER Ca^{2+} homeostasis, leading to abnormally high levels of Ca^{2+} stored in ER.

Furthermore, we examined whether the effects of PS1 on ER Ca^{2+} storage are γ-secretase activity dependent. Applying 1 μM L-685,458, a γ-secretase inhibitor, did not change the ER Ca^{2+} levels in PS-null MEF expressing GFP, GFP-$PS1^{wt}$ or GFP-$PS1^{G206D}$ as analyzed by two-away ANOVA (Fig. 3e, f). Together, out result indicates that the G206D mutation reduces the ability of PS1 to maintain ER Ca^{2+} homeostasis and this effect is independent of γ-secretase activity.

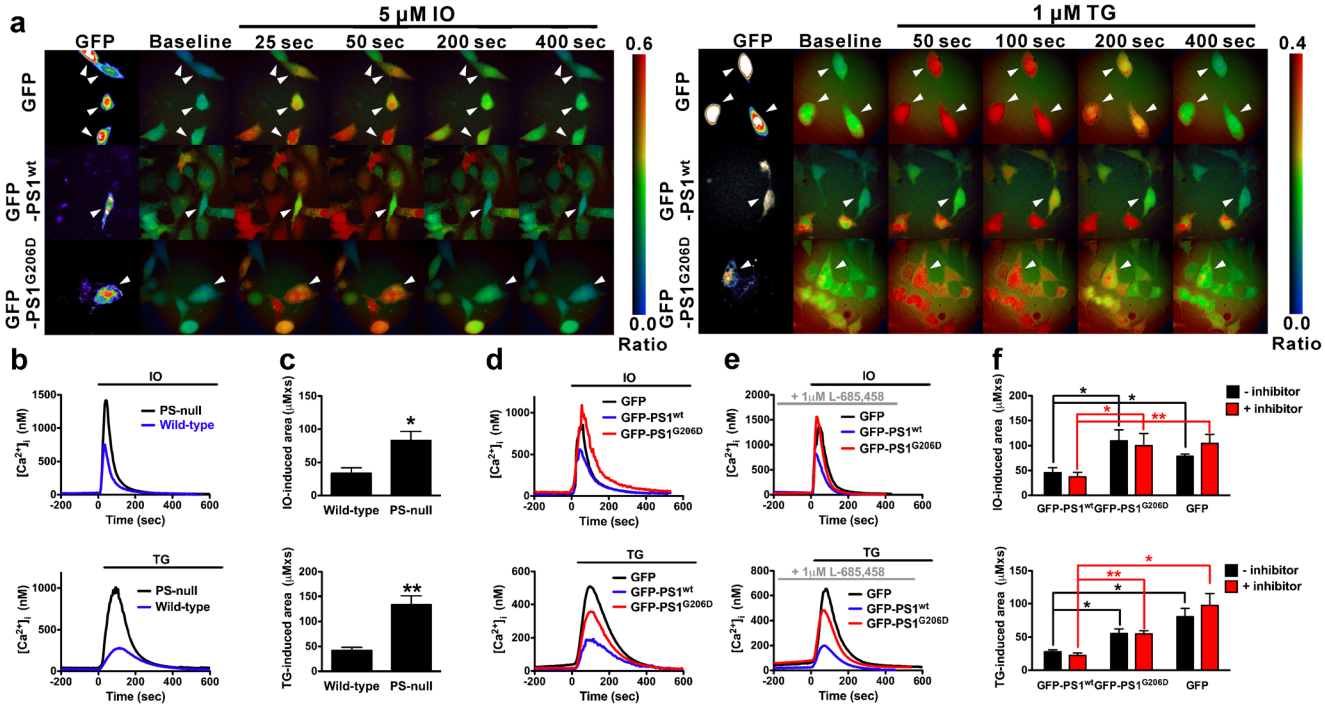

Fig. 3 The PS1 G206D mutation increased ER Ca^{2+} storage. ER Ca^{2+} storage was depleted by ionomycine (IO) or thapsigargin (TG). IO or TG was added at t=0 and monitored for 600 s. **a** Representative 340/380 Fura-2 images show the IO- (*left panel*) or TG- (*right panel*) induced Ca^{2+} responses in PS-null MEF transfected with GFP (*first row*), GFP-$PS1^{wt}$ (*second row*), and GFP-$PS1^{G206D}$ (*third row*). The transfected cells are indicated by *arrowheads*. The pseudo-color calibration scales for 340/380 ratios are shown on the right. **b** The Ca^{2+} signals evoked by IO or TG in PS-null and wild-type MEF. **c** The area under curve in **b** indicated higher ER Ca^{2+} in PS-null MEF. **d** The Ca^{2+} signals evoked by IO or TG in GFP, GFP-$PS1^{wt}$, or GFP-$PS1^{G206D}$ expressing cells. **e** The Ca^{2+} signals evoked by IO or TG in transfected cells in the presence of γ-secretase inhibitor, 1 μM L-685,458, are shown. **f** The area under curve in **d** (−*inhibitor*) and in **e** (+*inhibitor*). Only $PS1^{wt}$, but not $PS1^{G206D}$, can rescue the high ER Ca^{2+} in PS-null MEF. This effect was independent of γ-secretase activity. All the curves are shown as the average from each transfection. All data in the bar graphs are shown as mean±SEM ($n \geq 3$ independent transfection; $^*p<0.05$, $^{**}p<0.01$ vs. wild-type MEF or GFP-$PS1^{wt}$ by t test and ANOVA)

The G206D Mutation Alters PS1 Localization in ER and Early Endosome

One of the potential factors dysregulating ER Ca^{2+} in $PS1^{G206D}$-expressing cell is the reduction of PS1 in ER. To examine whether the G206D mutation affects the localization of PS1 in ER, we analyzed the percentage of co-localization of PS1 with Sec61β, an ER marker [58]. Same as other report [12], PS1 expression was mainly overlapped with ER markers. Ratio of Sec61β overlapping with $PS1^{G206D}$ (0.89 ±0.082) was significantly lower than that with $PS1^{wt}$ (set as 1) (Fig. 4a), suggesting that the G206D mutation reduces PS1 localization in ER.

γ-Secretase processing of APP is highlighted in the endosome-lysosome system [12, 59]. To evaluate whether the G206D mutation affects the localization of PS1 in endosome, we analyzed the percentage of co-localization of PS1 with Rab5, an early endosome marker [60]. Ratio of Rab5 overlapping with $PS1^{G206D}$ (1.43±0.433) was significantly higher than that with $PS1^{wt}$ (set as 1) (Fig. 4b), suggesting that the G206D mutation promotes the PS1 localization in early endosome. Together, our results indicate that the G206D mutation affects the cellular sorting of PS1, which is reduced in ER and increased in early endosome.

To further confirm our immunostaining result, we performed cellular organelle fractionation to compare the level of PS1 in different cellular compartments. In the ER-enriched fraction, the PS1-NTF level in $PS1^{G206D}$-expressing cells (0.84±0.029) was lower than that in $PS1^{wt}$-expressing cells (set as 1) (Fig. 4c). In addition, the ER-enriched fraction was further separated by Optiprep™ density gradient. The distribution of $PS1^{wt}$ was similar to the ER marker, ERp72, while the distribution of $PS1^{G206D}$ spread out to the fractions with ERp72 or with early endosome marker, Rab5 (Fig. 4d). The cellular organelle fractionation data further confirm our result that the G206D mutation decreases PS1 levels in ER but increases that in early endosome.

The decrease of $PS1^{G206D}$ in the ER may due to that this mutation causes PS1 misfolding and degraded by ER-associated degradation (ERAD). Thus, we compared the stability of PS1 holoprotein. Transfected cells were treated with cycloheximide (CHX), a protein synthesis inhibitor, and lysed after 1, 2, 4, 8, 12 h (ESM Fig. 2a). The levels of PS1 holoprotein were normalized to

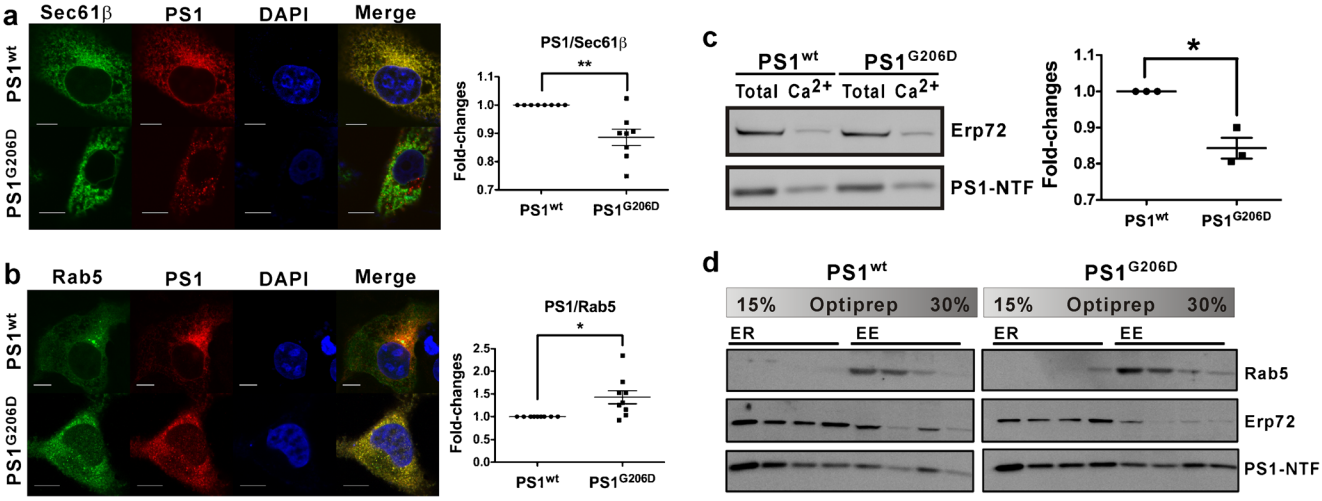

Fig. 4 The PS1 G206D mutation decreased PS1 levels in ER but increased PS1 levels in early endosome (EE). **a**, **b** PS1 variants (*red*) were co-transfected with GFP-Sec61β or GFP-Rab5 (*green*) into COS7 cells. **a** Fold-change of Sec61β overlapping with $PS1^{G206D}$ was significantly less than that with $PS1^{wt}$. **b** Fold-change of Rab5 overlapping with $PS1^{G206D}$ was significantly more than that with $PS1^{wt}$. Confocal images were selected from a single z-section. Each *dot* represents an average from one independent transfection (5–25 cells counted per transfection). **c**, **d** ER-enriched fraction was purified by centrifugation and $CaCl_2$ precipitation. **c** Examination of ER-enriched fraction and total cell lysate by Western blotting. Quantification result is shown by the normalization of PS1 in ER fraction/PS1 in total lysate/ER marker (ERp72) in ER fraction. The $PS1^{G206D}$ had less PS1 in the ER-enriched fraction. **d** Organelles in the ER-enriched fraction were further separated by Optiprep™ density gradient. The density of Optiprep™ was shown as indicated. The $PS1^{wt}$-NTF was concentrated in the ER fraction but the $PS1^{G206D}$-NTF was equally distributed in both ER and EE (*early endosome*) fractions, indicating that the percentage of $PS1^{G206D}$ is less in ER but more in EE. *Scale bar*, 10 μm. $^*p<0.05$, $^{**}p<0.01$ by *t* test

GAPDH and the levels of that at 0 h in each group were set as 1. $PS1^{G206D}$ holoprotein was less stable than $PS1^{wt}$ at 2 h after CHX treatment, but overall stability between these two proteins did not have significant difference (ESM Fig. 2b).

Effect of the G206D Mutation on Lysosomal Calcium and Autophagy

Deficiency of PS1 also leads to the accumulation of autophagosome and lower lysosomal Ca^{2+} storage [25, 34, 38]. Here, we dissected the autophagosome maturation process by using DsRed-GFP-LC3 reporter [50]. Green fluorescence reflects autophagosomes that did not fuse with lysosomes while red fluorescence reflects all autophagosomes and autolysosomes. The higher ratio of GFP to DsRed fluorescence indicates more autophagosome accumulation. Our result that the relative change of GFP to DsRed fluorescence in PS-null MEF (1.26±0.072) was significantly higher than that in control MEF (set as 1) (Fig. 5a), indicating the accumulation of autophagosome in PS deficient cells. To examine whether the G206D mutation affects autophagosome maturation process, we co-transfected $PS1^{wt}$ or $PS1^{G206D}$ with DsRed-GFP-LC3 reporter into PS-null MEF. The GFP to DsRed fluorescence ratio showed no difference between $PS1^{wt}$-expressing cells (set as 1) and $PS1^{G206D}$-expressing cells (0.87±0.057) (Fig. 5b), indicating that the G206D mutation does not affect the autophagosome maturation in the PS1 overexpression system.

The failure fusion of lysosome with autophagosome in PS1-deficient cells might be caused by the low lysosomal Ca^{2+} storage [36]. Therefore, we monitored the lysosomal Ca^{2+} release by treating Fura-2-loaded MEFs with Gly-Phe-β-naphtylamide (GPN), which causes osmotic lysis of cathepsin C-positive lysosomes. Application of 500 μM GPN evoked larger areas under curves in the control MEF compared with the PS-null MEF (Fig. 5c). The average size of GPN-sensitive Ca^{2+} pools in control MEF (13.84±1.561 μM×s) was significantly larger than PS-null MEF (9.21±1.361 μM×s) (Fig. 5d), which is consistent with previous reports on the decreasing of lysosomal Ca^{2+} in the PS-deficient cells [38, 39].

To examine whether $PS1^{G206D}$ lowers lysosomal Ca^{2+} level, we transfected GFP-$PS1^{wt}$ or GFP-$PS1^{G206D}$ into PS-null MEF. Because we found that Lipofectamine™ may interfere with lysosomal Ca^{2+}, we used the TurboFect™ transfection reagent to examine the GPN-evoked Ca^{2+} signals. The GPN-evoked Ca^{2+} signal in the GFP-$PS1^{wt}$-expressing cells (10.00±1.745 μM×s) was similar with that in the GFP-$PS1^{G206D}$-expressing cells (8.08±1.405 μM×s) (Fig. 5e, f). Our result suggests that $PS1^{G206D}$ does not affect lysosomal Ca^{2+} homeostasis.

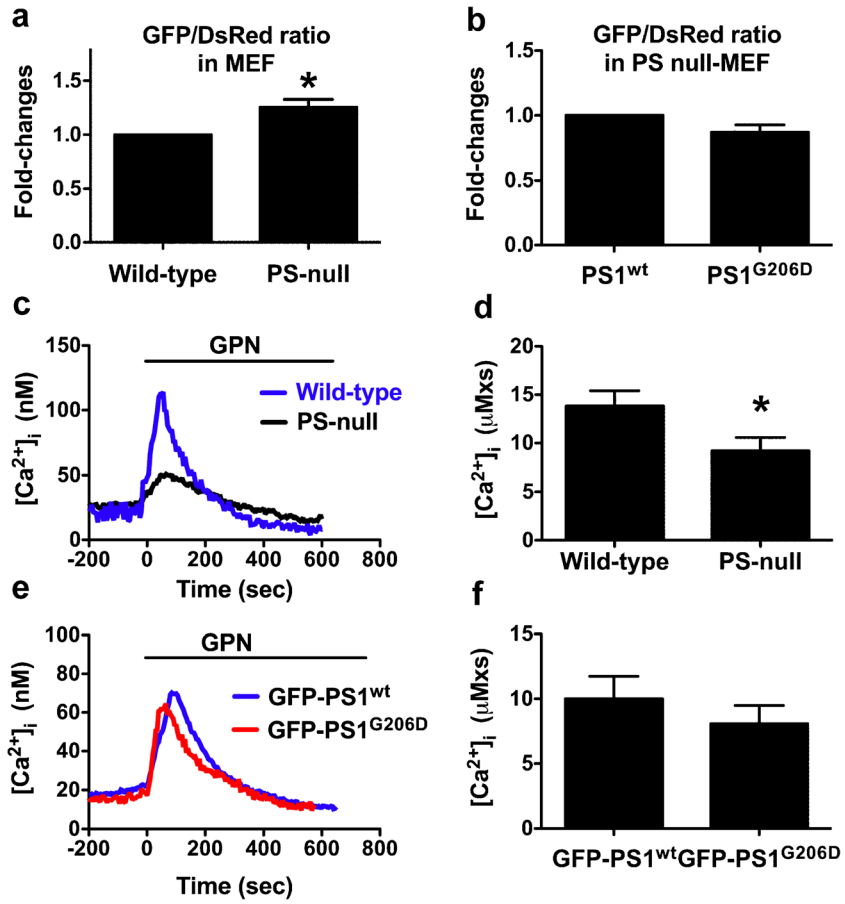

Fig. 5 The PS1 G206D mutation did not affect autophagosome maturation and lysosomal Ca^{2+} storage. **a**, **b** Accumulation of autophagosome was monitored by the GFP-DsRed-LC3 reporter. The ratio of GFP to DsRed fluorescence intensity was normalized to the wild-type control. **a** PS-null MEF had significantly higher ratio of GFP to DsRed than the wild-type MEF, indicating more autophagosome accumulation. **b** The ratio of GFP to DsRed was similar between $PS1^{wt}$ and $PS1^{G206D}$-transfected MEF. **c**-**f** Lysosomal Ca^{2+} was released by GPN and monitored by Fura-2 in MEF. **c** The Ca^{2+} signals evoked by GPN in PS-null and wild-type MEF. **d** The area under curve in **c** indicates lower lysosomal Ca^{2+} in PS-null MEF. **e** The Ca^{2+} signals evoked by GPN in GFP-$PS1^{wt}$ or GFP-$PS1^{G206D}$ expressing PS1-null MEF. **f** The area under curve in **e** had no significant difference between groups. All the curves are shown as the average from each transfection. All data in the *bar graphs* are shown as mean±SEM ($n \geq 3$ independent transfection; *$p<0.05$ by *t* test)

The G206D Mutation Did Not Affect Cell Death Rate Under Oxidative Stress

Some of the PS1 FAD mutants increase cell death under oxidative stress [61, 62]. Thus, we measured cell death by DNA fragmentation and induced oxidative stress by H_2O_2. The DNA fragmentation was measured by TUNEL assay and PI staining in GFP or GFP-PS1-transfected HEK293T cells. For TUNEL assay, after 24-h treatment of 1,500 μM H_2O_2, the percentage of transfected cells with TUNEL-positive signal (Q2/(Q2+Q3)) had no significant difference between GFP-$PS1^{wt}$ (0.593±0.274-fold of GFP control) and GFP-$PS1^{G206D}$ (0.721±0.116-fold of GFP control) transfected cells (Fig. 6a, b). This result indicates that the G206D mutation does not affect the percentage of TUNEL-positive cells under oxidative stress.

For PI staining, the presence of sub-G1 phase indicates DNA fragmentation and is defined as dead cells [63]. After treatment of H_2O_2, the sub-G1 population was increased in all groups compared to each untreated control (Fig. 6c, d), but there was no difference between GFP-$PS1^{wt}$ (2.79±1.288-fold higher than untreated control) and GFP-$PS1^{G206D}$ (2.56±0.462-fold higher than untreated control) transfected cells. This result indicates that H_2O_2 can induce cell death, but the G206D mutation does not affect the rate of H_2O_2-induced cell death.

Interestingly, under oxidative stress, GFP-PS1-transfected groups had more cells in G1 phase ($PS1^{wt}$, 1.051±0.051; $PS1^{G206D}$, 1.112±0.11) (Fig. 6e) and less cells in G2 phase ($PS1^{wt}$, 0.784±0.216; $PS1^{G206D}$, 0.745±0.255) (Fig. 6g) and no difference in S phase (Fig. 6f) compared to the GFP-transfected group (G1, 0.819±0.182; G2, 1.113±0.113). This result indicates that overexpression of either GFP-$PS1^{wt}$ or

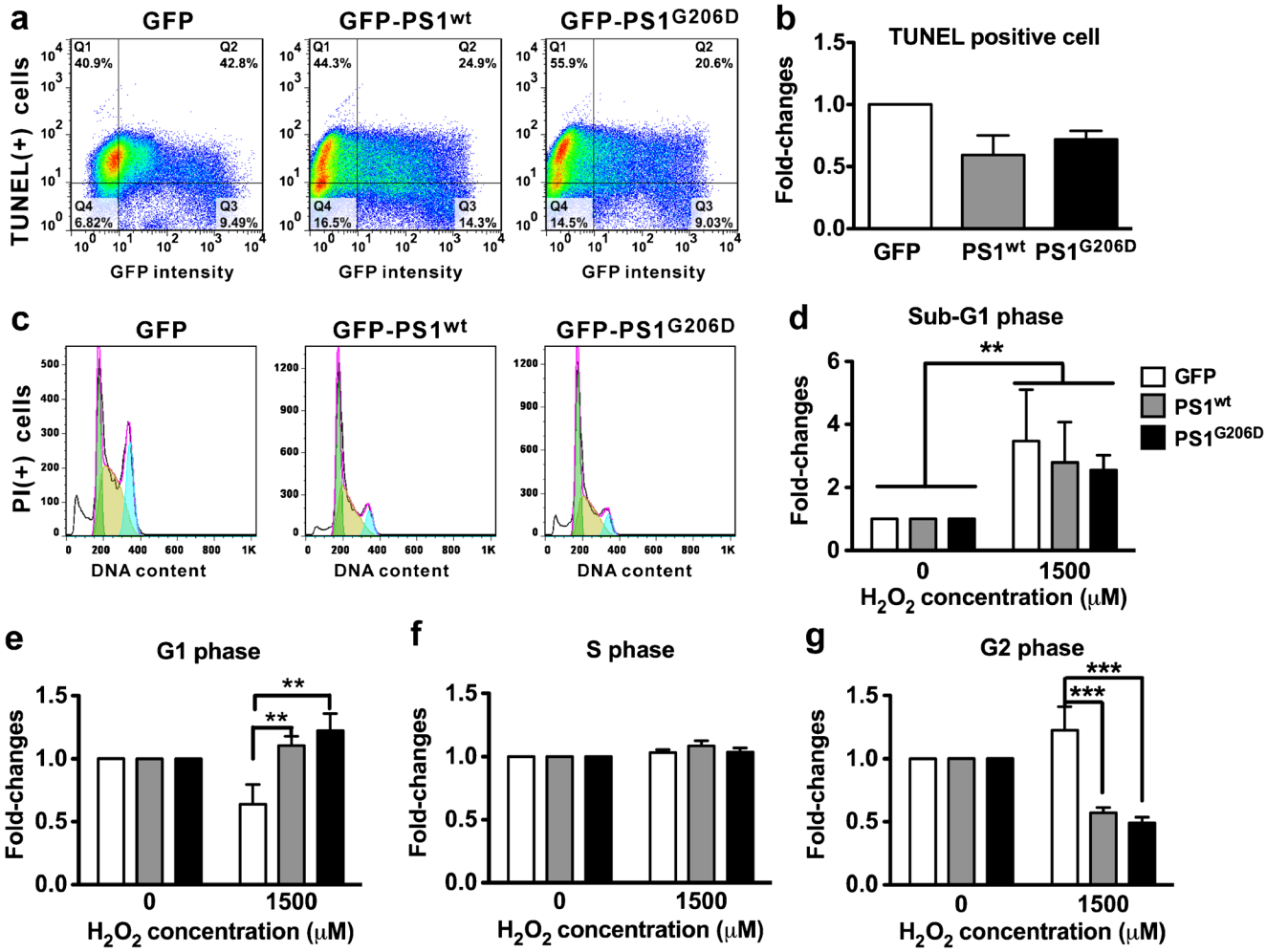

Fig. 6 The PS1 G206D mutation did not alter survival response under oxidative stress. **a**, **b** Overexpression of either GFP-PS1^{wt} or GFP-PS1^{G206D} had a similar trend to reduce TUNEL-positive cells under 1500 μM H_2O_2. **c** Cell cycle analysis was reported by PI staining and flow cytometry. **d** The H_2O_2 treatment increased the cell having sub-G1 phase, which had no significant difference among transfected cells. **e**–**g** Overexpression of GFP-PS1^{wt} or GFP-PS1^{G206D} had a similar trend to increase G1 phase **e** and to reduce G2 phase **f** and no effect on S phase **g** compared with the control group. All data in the bar graphs are shown as mean±SEM ($n \geq 3$ independent transfection; *$p<0.05$, **$p<0.01$ by ANOVA)

GFP-PS1^{G206D} induces cell cycle arrest under oxidative stress. Together, our results suggest that the G206D mutation does not affect cell death under oxidative stress.

Discussion

In this study, we demonstrated that the G206D mutation reduced the PS1-Pen2 interaction but did not alter PS1 endoproteolysis, suggesting that γ-secretase could be assembled and activated. PS1^{G206D} increased the $A\beta_{42}$ to $A\beta_{total}$ ratio, which might promote the formation of toxic $A\beta_{42}$ oligomers. Furthermore, PS1^{G206D} increased the ER Ca^{2+} storage but did not affect lysosomal function, indicating that the PS1 regulation in ER Ca^{2+} homeostasis might not directly link to that in lysosome. Although PS1^{G206D} did not directly contribute to cell death, both the increase of $A\beta_{42}$ proportion and the dysregulation of ER Ca^{2+} have been implicated in the etiology of AD.

Effects of the G206D Mutation on γ-Secretase Formation and Activity

The formation and activation of γ-secretase are tightly controlled by ER-Golgi recycling regulators and ER retention signals to ensure that only fully assembled γ-secretase leaves ER [64–66]. PS1 contains at least two ER retention signals: one in the proximal end of PS1 CTF [64] and the other in the transmembrane domain 4 (TMD4) of PS1 NTF [13], in which the G206D mutation is located [14–16]. The interaction between Pen2 and PS1TMD4 is required for fully assembled γ-

secretase to leave ER [13]. In our findings, the reduced $PS1^{G206D}$-Pen2 interaction and less $PS1^{G206D}$ level in ER suggest that the G206D mutation might only contribute to minor conformational changes, but not abolishes the γ-secretase formation and ER export. The normal $PS1^{G206D}$ endoproteolysis also indicates the γ-secretase activation.

The rate of ER export and protein degradation could contribute to the reduced $PS1^{G206D}$ level in ER. The $PS1^{G206D}$ has an additional polar transmembrane residue, which may regulate both ER export and protein degradation [67]. A single mutation in polar amino acid N204 is sufficient to disrupt ER export, PS1-Pen2 interaction and γ-secretase activation [16]. However, the G206D mutation increased ER export, partially reduced the PS1-Pen2 interaction, and had no effect on γ-secretase activation. This difference may be due to that the G206D contributes an additional polar residue located at the opposite position to the N204 in TMD4.

In our findings, the PS1 G206D mutation increased the ratio of $A\beta_{42}/A\beta_{total}$ but had no influence on the ratio of NICD/Notch, indicating that this mutation has effects on γ-cleavage but not ε-cleavage. The increased $A\beta_{42}$ proportion could be due to the PS1 conformational changes [68, 69]. In previous reports, PS1 conformational changes induced by elongation of Pen2 N terminus shows effects on γ-cleavage but not ε-cleavage, thus causes $A\beta_{42}$ overproduction [70]. Also, the majority of PS1 mutations have independent effects on γ-cleavage and ε-cleavage [18, 53, 54]. Loss of ε-cleavage on Notch, Erb4, N-Cadherin, and APP is less observed among PS1 FAD mutants, but the impairment of the consecutive γ-cleavage on Aβ and increase of $A\beta_{42}$ ratio is conserved in PS1 FAD mutants [18].

The G206D Mutation Increased ER Ca^{2+} Storage Without Apparent Effects on Lysosomal Function

Deficiency of PS1 results in ER Ca^{2+} overload, leading to the excess intracellular Ca^{2+} release from ER after cellular signaling stimulation [24, 26, 27]. Presence of excess intracellular Ca^{2+} from ER induces synaptic dysfunction [30–33], and perturbation in Ca^{2+} homeostasis affects Aβ generation [57, 71]. Therefore, ER Ca^{2+} overload has been implicated as a causative factor for the early pathological changes in AD [31–33], and normalization of intracellular Ca^{2+} homeostasis could be a strategy for the development of effective disease-modifying therapies.

Autophagosome accumulation is involved in the pathogenesis of AD [72]. How could PS deficiency lead to autophagosome accumulation? Autophagosome accumulation could be caused by the disruption of lysosomal acidification or the failure of lysosomal Ca^{2+} release during the fusion of lysosome and autophagosome. One possibility is that PS1 acts as a chaperon of the V0a1 ATPase and thus directly affects the lysosomal acidification [25, 73]. However, several groups did not observe the lysosomal acidification defects [34, 38, 74]. The other possibility is that lysosomal Ca^{2+} storage may be indirectly affected by the PS-induced impairment of ER Ca^{2+} homeostasis [37]. More investigations are needed to elucidate the mechanism of the higher autophagosome accumulation in the PS-null cells. However, the G206D mutation only affects ER Ca^{2+}, but not lysosomal Ca^{2+} and autophagy maturation process in our system. Our result indicates that the PS1 regulation in ER and lysosomal function might not be fully correlated.

Subcellular Distribution of PS1 Altered by the G206D Mutation

The alteration of $PS1^{G206D}$ subcellular distribution might help to explain the γ-secretase-dependent and -independent deficits of this mutant. Intracellular PS1 is distributed in two pools: a major pool in ER and a minor pool in trans-Golgi network, plasma membrane, and endosomes [10, 11]. Our result indicates that the ER Ca^{2+} overload might be due to the decreased level of $PS1^{G206D}$ in ER (Fig. 5). We also found the increased level of $PS1^{G206D}$ in early endosome (Fig. 5), where the active form of γ-secretase for APP processing is found [75], that might correlate with the increased ratio of $A\beta_{42}$ in $PS1^{G206D}$-expressing cells. However, due to the approach we used, it is hard to distinguish whether the holoprotein or NTF is responsible for these changes.

The G206D Mutation Did Not Alter Cell Survival Under Oxidative Stress

Although $PS1^{G206D}$ increased ER Ca^{2+} storage, the G206D mutation did not accelerate cell death under oxidative stress. Nonetheless, effect of PS1 FAD mutations on cell survival is dependent on experimental system, amino acid substitution, and stress type. Under different experimental systems, the same PS1 mutant could show diverse consequences. For example, the PS1 P264L mutation had no effect on tunicamycin-induced cell death in the P264L knock-in mice [76], but it promoted caspase 3 signaling when expressed in primary neurons [40]. Moreover, the stress type plays an important role in the consequence of cell survival. For example, the PS1 L286V mutant rendered neuronal vulnerability to isoflurane toxicity, but not sevoflurane or desflurane toxicity [77]. Therefore, we cannot exclude the possibility that the G206D mutation could alter the cell survival in the other experimental systems.

Overexpressing $PS1^{wt}$ or $PS1^{G206D}$ leads to cell cycle arrest at G1 phase under oxidative stress (Fig. 5e) [78, 79]. A possible mechanism of PS1-induced arrest is mediated through the abnormal activation of Notch, which arrests cells in the G1 phase by preventing Wnt-induced G2 arrest [80]. Because the PS1 G206D mutation did not alter γ-secretase

activity toward Notch (Fig. 2d, e), PS1-induced G1 arrest might be due to the over-activation of Notch via high level of $PS1^{wt}$ or $PS1^{G206D}$.

Conclusion

There are three other mutations found at this location including G206A [81], G206S [82], and G206V [83], implying that mutations at this G206 position may have a great impact on AD pathogenesis. According to bioinformatics analysis on the FAD-linked PS1 mutations, the amino acid G206 is a highly conserved amino acid among 14 species and mutation from glycine into aspartic acid has more potential to damage PS1 activity in three functional significance analyses [84]. Here, we found that both increased $A\beta_{42}$ proportion and the ER Ca^{2+} storage are the pathogenic mechanisms underlying the FAD-linked PS1 G206D mutation. Our finding also promotes the understanding of PS1-Pen2 interaction in the etiology of AD.

Acknowledgments We thank Dr. De Strooper for providing PS-null MEF, Dr. Yung-Feng Liao for providing HA-Aph1, Flag-Pen2, wild-type human PS1, and DsRed-GFP-LC3-expressing plasmids, Dr. Liang-Tung Yang for providing NotchΔmyc- and V/LΔmyc-expressing plasmids, and Dr. Rey-Huei Chen for EGFP-Sec61β and EGFP-Rab5 expressing plasmids. This work is supported by Taiwan Ministry of Science and Technology grant (NSC 102-2320-B-010-021-MY2), National Health Research Institute (NHRI-EX98-9816NC), Cheng Hsin General Hospital (102F218C05), Yen Tjing Ling Medical Foundation (CI-102-4), Taipei Veterans General Hospital grant (V103E4-002), and Taiwan Ministry of Education Aim for Top University Grant.

Conflict of Interest The authors declare that they have no competing interests.

Author Contributions I.H.C. designed research and analyzed data; W.T.C., Y.F.H., Y.J.H., C.C.L., and Y.T.L. performed research and analyzed data; Y.C.L. and C.C.L. helped with Ca^{2+} imaging analysis; and W.T.C. and I.H.C. wrote the paper.

References

1. Querfurth HW, LaFerla FM (2010) Alzheimer's disease. N Engl J Med 362(4):329–344. doi:10.1056/NEJMra0909142
2. Hardy J, Selkoe DJ (2002) The amyloid hypothesis of Alzheimer's disease: progress and problems on the road to therapeutics. Science 297(5580):353–356. doi:10.1126/science.1072994
3. Roher AE, Lowenson JD, Clarke S, Woods AS, Cotter RJ, Gowing E, Ball MJ (1993) b-Amyloid-(1–42) is a major component of cerebrovascular amyloid deposits: implications for the pathology of Alzheimer disease. Proc Natl Acad Sci U S A 90:10836–10840. doi:10.1073/pnas.90.22.10836
4. McGowan E, Pickford F, Kim J, Onstead L, Eriksen J, Yu C, Skipper L, Murphy MP, Beard J, Das P, Jansen K, Delucia M, Lin WL, Dolios G, Wang R, Eckman CB, Dickson DW, Hutton M, Hardy J, Golde T (2005) Ab42 is essential for parenchymal and vascular amyloid deposition in mice. Neuron 47(2):191–199. doi:10.1016/j.neuron.2005.06.030
5. Edbauer D, Winkler E, Regula JT, Pesold B, Steiner H, Haass C (2003) Reconstitution of g-secretase activity. Nat Cell Biol 5(5):486–488. doi:10.1038/ncb960
6. Takasugi N, Tomita T, Hayashi I, Tsuruoka M, Niimura M, Takahashi Y, Thinakaran G, Iwatsubo T (2003) The role of presenilin cofactors in the gamma-secretase complex. Nature 422(6930):438–441. doi:10.1038/nature01506
7. De Strooper B, Annaert W, Cupers P, Saftig P, Craessaerts K, Mumm JS, Schroeter EH, Schrijvers V, Wolfe MS, Ray WJ, Goate A, Kopan R (1999) A presenilin-1-dependent gamma-secretase-like protease mediates release of Notch intracellular domain. Nature 398(6727):518–522. doi:10.1038/19083
8. De Strooper B, Saftig P, Craessaerts K, Vanderstichele H, Guhde G, Annaert W, Von Figura K, Van Leuven F (1998) Deficiency of presenilin-1 inhibits the normal cleavage of amyloid precursor protein. Nature 391:387–390. doi:10.1038/34910
9. Herreman A, Hartmann D, Annaert W, Saftig P, Craessaerts K, Serneels L, Umans L, Schrijvers V, Checler F, Vanderstichele H, Baekelandt V, Dressel R, Cupers P, Huylebroeck D, Zwijsen A, Van Leuven F, De Strooper B (1999) Presenilin 2 deficiency causes a mild pulmonary phenotype and no changes in amyloid precursor protein processing but enhances the embryonic lethal phenotype of presenilin 1 deficiency. Proc Natl Acad Sci U S A 96(21):11872–11877. doi:10.1073/pnas.96.21.11872
10. Rechards M, Xia W, Oorschot VM, Selkoe DJ, Klumperman J (2003) Presenilin-1 exists in both pre- and post-Golgi compartments and recycles via COPI-coated membranes. Traffic 4(8):553–565. doi:10.1034/j.1600-0854.2003.t01-1-00114.x
11. Haass C, Kaether C, Thinakaran G, Sisodia S (2012) Trafficking and proteolytic processing of APP. Cold Spring Harb Perspect Med 2(5):a006270. doi:10.1101/cshperspect.a006270
12. Cupers P, Bentahir M, Craessaerts K, Orlans I, Vanderstichele H, Saftig P, De Strooper B, Annaert W (2001) The discrepancy between presenilin subcellular localization and gamma-secretase processing of amyloid precursor protein. J Cell Biol 154(4):731–740. doi:10.1083/jcb.200104045
13. Fassler M, Zocher M, Klare S, de la Fuente AG, Scheuermann J, Capell A, Haass C, Valkova C, Veerappan A, Schneider D, Kaether C (2010) Masking of transmembrane-based retention signals controls ER export of gamma-secretase. Traffic 11(2):250–258. doi:10.1111/j.1600-0854.2009.01014.x
14. Kim SH, Sisodia SS (2005) Evidence that the "NF" motif in transmembrane domain 4 of presenilin 1 is critical for binding with PEN-2. J Biol Chem 280(51):41953–41966. doi:10.1074/jbc.M509070200
15. Watanabe N, Tomita T, Sato C, Kitamura T, Morohashi Y, Iwatsubo T (2005) Pen-2 is incorporated into the gamma-secretase complex through binding to transmembrane domain 4 of presenilin 1. J Biol Chem 280(51):41967–41975. doi:10.1074/jbc.M509066200
16. Fassler M, Li X, Kaether C (2011) Polar transmembrane-based amino acids in presenilin 1 are involved in endoplasmic reticulum localization, Pen2 protein binding, and gamma-secretase complex stabilization. J Biol Chem 286(44):38390–38396. doi:10.1074/jbc.M111.252429
17. Takami M, Nagashima Y, Sano Y, Ishihara S, Morishima-Kawashima M, Funamoto S, Ihara Y (2009) gamma-Secretase: successive tripeptide and tetrapeptide release from the transmembrane domain of beta-carboxyl terminal fragment. J Neurosci 29(41):13042–13052. doi:10.1523/JNEUROSCI.2362-09.2009
18. Chavez-Gutierrez L, Bammens L, Benilova I, Vandersteen A, Benurwar M, Borgers M, Lismont S, Zhou L, Van Cleynenbreugel S, Esselmann H, Wiltfang J, Serneels L, Karran E, Gijsen H, Schymkowitz J, Rousseau F, Broersen K, De Strooper B (2012) The mechanism of gamma-Secretase dysfunction in familial

Alzheimer disease. EMBO J 31(10):2261–2274. doi:10.1038/emboj.2012.79
19. Weidemann A, Eggert S, Reinhard FB, Vogel M, Paliga K, Baier G, Masters CL, Beyreuther K, Evin G (2002) A novel epsilon-cleavage within the transmembrane domain of the Alzheimer amyloid precursor protein demonstrates homology with Notch processing. Biochemistry 41(8):2825–2835. doi:10.1021/bi015794o
20. Sastre M, Steiner H, Fuchs K, Capell A, Multhaup G, Condron MM, Teplow DB, Haass C (2001) Presenilin-dependent gamma-secretase processing of beta-amyloid precursor protein at a site corresponding to the S3 cleavage of Notch. EMBO Rep 2(9):835–841. doi:10.1093/embo-reports/kve180
21. Shen J, Bronson RT, Chen DF, Xia W, Selkoe DJ, Tonegawa S (1997) Skeletal and CNS defects in presenilin-1-deficient mice. Cell 89:629–639. doi:10.1016/S0092-8674(00)80244-5
22. Wong PC, Zheng H, Chen H, Becher MW, Sirinathsinghji DJ, Trumbauer ME, Chen HY, Price DL, Van der Ploeg LH, Sisodia SS (1997) Presenilin 1 is required for Notch1 and DII1 expression in the paraxial mesoderm. Nature 387:288–292. doi:10.1038/387288a0
23. Shen J, Kelleher RJ 3rd (2007) The presenilin hypothesis of Alzheimer's disease: evidence for a loss-of-function pathogenic mechanism. Proc Natl Acad Sci U S A 104(2):403–409. doi:10.1073/pnas.0608332104
24. Tu H, Nelson O, Bezprozvanny A, Wang Z, Lee S-F, Hao Y-H, Serneels L, De Strooper B, Yu G, Bezprozvanny I (2006) Presenilins form ER Ca^{2+} leak channels, a function disrupted by familial Alzheimer's disease-linked mutations. Cell 126(5):981–993. doi:10.1016/j.cell.2006.06.059
25. Lee JH, Yu WH, Kumar A, Lee S, Mohan PS, Peterhoff CM, Wolfe DM, Martinez-Vicente M, Massey AC, Sovak G, Uchiyama Y, Westaway D, Cuervo AM, Nixon RA (2010) Lysosomal proteolysis and autophagy require presenilin 1 and are disrupted by Alzheimer-related PS1 mutations. Cell 141(7):1146–1158. doi:10.1016/j.cell.2010.05.008
26. Chan SL, Mayne M, Holden CP, Geiger JD, Mattson MP (2000) Presenilin-1 mutations increase levels of ryanodine receptors and calcium release in PC12 cells and cortical neurons. J Biol Chem 275(24):18195–18200. doi:10.1074/jbc.m000040200
27. Stutzmann GE, Caccamo A, LaFerla FM, Parker I (2004) Dysregulated IP_3 signaling in cortical neurons of knock-in mice expressing an Alzheimer's-linked mutation in presenilin1 results in exaggerated Ca^{2+} signals and altered membrane excitability. J Neurosci 24(2):508–513. doi:10.1523/JNEUROSCI.4386-03.2004
28. Bandara S, Malmersjo S, Meyer T (2013) Regulators of calcium homeostasis identified by inference of kinetic model parameters from live single cells perturbed by siRNA. Sci Signal 6(283):ra56. doi:10.1126/scisignal.2003649
29. Bezprozvanny I (2013) Presenilins and calcium signaling-systems biology to the rescue. Sci Signal 6(283):pe24. doi:10.1126/scisignal.2004296
30. Sun S, Zhang H, Liu J, Popugaeva E, Xu NJ, Feske S, White CL 3rd, Bezprozvanny I (2014) Reduced synaptic STIM2 expression and impaired store-operated calcium entry cause destabilization of mature spines in mutant presenilin mice. Neuron 82(1):79–93. doi:10.1016/j.neuron.2014.02.019
31. Schneider I, Reversé D, Dewachter I, Ris L, Caluwaerts N, Kuipéri C, Gilis M, Geerts H, Kretzschmar H, Godaux E, Moechars D, Van Leuven F, Herms J (2001) Mutant presenilins disturb neuronal calcium homeostasis in the brain of transgenic mice, decreasing the threshold for excitotoxicity and facilitating long-term potentiation. J Biol Chem 276:11539–11544. doi:10.1074/jbc.M010977200
32. Goussakov I, Miller MB, Stutzmann GE (2010) NMDA-mediated Ca(2+) influx drives aberrant ryanodine receptor activation in dendrites of young Alzheimer's disease mice. J Neurosci 30(36):12128–12137. doi:10.1523/JNEUROSCI.2474-10.2010
33. Wu B, Yamaguchi H, Lai FA, Shen J (2013) Presenilins regulate calcium homeostasis and presynaptic function via ryanodine receptors in hippocampal neurons. Proc Natl Acad Sci U S A 110(37):15091–15096. doi:10.1073/pnas.1304171110
34. Neely KM, Green KN, LaFerla FM (2011) Presenilin is necessary for efficient proteolysis through the autophagy-lysosome system in a gamma-secretase-independent manner. J Neurosci 31(8):2781–2791. doi:10.1523/JNEUROSCI.5156-10.2010
35. Luzio JP, Bright NA, Pryor PR (2007) The role of calcium and other ions in sorting and delivery in the late endocytic pathway. Biochem Soc Trans 35(Pt 5):1088–1091. doi:10.1042/BST0351088
36. Saftig P, Klumperman J (2009) Lysosome biogenesis and lysosomal membrane proteins: trafficking meets function. Nat Rev Mol Cell Biol 10(9):623–635. doi:10.1038/nrm2745
37. Bezprozvanny I (2012) Presenilins: a novel link between intracellular calcium signaling and lysosomal function? J Cell Biol 198(1):7–10. doi:10.1083/jcb.201206003
38. Coen K, Flannagan RS, Baron S, Carraro-Lacroix LR, Wang D, Vermeire W, Michiels C, Munck S, Baert V, Sugita S, Wuytack F, Hiesinger PR, Grinstein S, Annaert W (2012) Lysosomal calcium homeostasis defects, not proton pump defects, cause endo-lysosomal dysfunction in PSEN-deficient cells. J Cell Biol 198(1):23–35. doi:10.1083/jcb.201201076
39. Neely Kayala KM, Dickinson GD, Minassian A, Walls KC, Green KN, Laferla FM (2012) Presenilin-null cells have altered two-pore calcium channel expression and lysosomal calcium: implications for lysosomal function. Brain Res 1489:8–16. doi:10.1016/j.brainres.2012.10.036
40. Baki L, Neve RL, Shao Z, Shioi J, Georgakopoulos A, Robakis NK (2008) Wild-type but not FAD mutant presenilin-1 prevents neuronal degeneration by promoting phosphatidylinositol 3-kinase neuroprotective signaling. J Neurosci 28(2):483–490. doi:10.1523/jneurosci.4067-07.2008
41. Tanzi R, Bertram L (2005) Twenty years of the Alzheimer's disease amyloid hypothesis: a genetic perspective. Cell 120:545–555. doi:10.1016/j.cell.2005.02.008
42. Wu Y-Y, Cheng IH-J, Lee C-C, Chiu M-J, Lee M-J, Chen T-F, Hsu J-L (2011) Clinical phenotype of G206D mutation in the presenilin 1 gene in pathologically confirmed familial Alzheimer's disease. J Alzheimers Dis 25(1):145–150. doi:10.3233/JAD-2011-102031
43. Raux G, Guyant-Maréchal L, Martin C, Bou J, Penet C, Brice A, Hannequin D, Frebourg T, Campion D (2005) Molecular diagnosis of autosomal dominant early onset Alzheimer's disease: an update. J Med Genet 42(10):793–795. doi:10.1136/jmg.2005.033456
44. Kuo LH, Hu MK, Hsu WM, Tung YT, Wang BJ, Tsai WW, Yen CT, Liao YF (2008) Tumor necrosis factor-alpha-elicited stimulation of gamma-secretase is mediated by c-Jun N-terminal kinase-dependent phosphorylation of presenilin and nicastrin. Mol Biol Cell 19(10):4201–4212. doi:10.1091/mbc.E07-09-0987
45. Tung YT, Wang BJ, Hsu WM, Hu MK, Her GM, Huang WP, Liao YF (2014) Presenilin-1 regulates the expression of p62 to govern p62-dependent Tau degradation. Mol Neurobiol 49(1):10–27. doi:10.1007/s12035-013-8482-y
46. Tung YT, Hsu WM, Lee H, Huang WP, Liao YF (2010) The evolutionarily conserved interaction between LC3 and p62 selectively mediates autophagy-dependent degradation of mutant huntingtin. Cell Mol Neurobiol 30(5):795–806. doi:10.1007/s10571-010-9507-y
47. Yang LT, Nichols JT, Yao C, Manilay JO, Robey EA, Weinmaster G (2005) Fringe glycosyltransferases differentially modulate Notch1 proteolysis induced by Delta1 and Jagged1. Mol Biol Cell 16(2):927–942. doi:10.1091/mbc.E04-07-0614
48. Tseng LC, Chen RH (2011) Temporal control of nuclear envelope assembly by phosphorylation of lamin B receptor. Mol Biol Cell 22(18):3306–3317. doi:10.1091/mbc.E11-03-0199

49. Grynkiewicz G, Poenie M, Tsien RY (1985) A new generation of Ca^{2+} indicators with greatly improved fluorescence properties. J Biol Chem 260(6):3440–3450
50. Kimura S, Noda T, Yoshimori T (2007) Dissection of the autophagosome maturation process by a novel reporter protein, tandem fluorescent-tagged LC3. Autophagy 3(5):452–460. doi:10.4161/auto.4451
51. Riccardi C, Nicoletti I (2006) Analysis of apoptosis by propidium iodide staining and flow cytometry. Nat Protoc 1(3):1458–1461. doi:10.1038/nprot.2006.238
52. Dean PN, Jett JH (1974) Mathematical analysis of DNA distributions derived from flow microfluorometry. J Cell Biol 60(2):523–527. doi:10.1083/jcb.60.2.523
53. Chen F, Gu Y, Hasegawa H, Ruan X, Arawaka S, Fraser P, Westaway D, Mount H, St George-Hyslop P (2002) Presenilin 1 mutations activate gamma 42-secretase but reciprocally inhibit epsilon-secretase cleavage of amyloid precursor protein (APP) and S3-cleavage of notch. J Biol Chem 277(39):36521–36526. doi:10.1074/jbc.M205093200
54. Moehlmann T, Winkler E, Xia X, Edbauer D, Murrell J, Capell A, Kaether C, Zheng H, Ghetti B, Haass C, Steiner H (2002) Presenilin-1 mutations of leucine 166 equally affect the generation of the Notch and APP intracellular domains independent of their effect on Abeta 42 production. Proc Natl Acad Sci U S A 99(12):8025–8030. doi:10.1073/pnas.112686799
55. Schroeter EH, Kisslinger JA, Kopan R (1998) Notch-1 signalling requires ligand-induced proteolytic release of intracellular domain. Nature 393(6683):382–386. doi:10.1038/30756
56. Shilling D, Mak DO, Kang DE, Foskett JK (2012) Lack of evidence for presenilins as endoplasmic reticulum Ca2+ leak channels. J Biol Chem 287(14):10933–10944. doi:10.1074/jbc.M111.300491
57. Green KN, Demuro A, Akbari Y, Hitt BD, Smith IF, Parker I, LaFerla FM (2008) SERCA pump activity is physiologically regulated by presenilin and regulates amyloid β production. J Cell Biol 181(7):1107–1116. doi:10.1083/jcb.200706171
58. Kalies KU, Rapoport TA, Hartmann E (1998) The beta subunit of the Sec61 complex facilitates cotranslational protein transport and interacts with the signal peptidase during translocation. J Cell Biol 141(4):887–894. doi:10.1083/jcb.141.4.887
59. Petanceska SS, Seeger M, Checler F, Gandy S (2000) Mutant presenilin 1 increases the levels of Alzheimer amyloid beta-peptide Abeta42 in late compartments of the constitutive secretory pathway. J Neurochem 74(5):1878–1884. doi:10.1046/j.1471-4159.2000.0741878.x
60. Gorvel JP, Chavrier P, Zerial M, Gruenberg J (1991) rab5 controls early endosome fusion in vitro. Cell 64(5):915–925. doi:10.1016/0092-8674(91)90316-q
61. Mohmmad Abdul H, Sultana R, Keller JN, St Clair DK, Markesbery WR, Butterfield DA (2006) Mutations in amyloid precursor protein and presenilin-1 genes increase the basal oxidative stress in murine neuronal cells and lead to increased sensitivity to oxidative stress mediated by amyloid beta-peptide (1–42), HO and kainic acid: implications for Alzheimer's disease. J Neurochem 96(5):1322–1335. doi:10.1111/j.1471-4159.2005.03647.x
62. Nakajima M, Miura M, Aosaki T, Shirasawa T (2001) Deficiency of presenilin-1 increases calcium-dependent vulnerability of neurons to oxidative stress in vitro. J Neurochem 78(4):807–814. doi:10.1046/j.1471-4159.2001.00478.x
63. Lizard G, Miguet C, Gueldry S, Monier S, Gambert P (1997) Flow cytometry measurement of DNA fragmentation in the course of cell death via apoptosis. New techniques for evaluation of DNA status for the pathologist. Ann Pathol 17(1):61–66. doi: AP-03-1997-17-1-0242-6498-101019-ART85
64. Kaether C, Capell A, Edbauer D, Winkler E, Novak B, Steiner H, Haass C (2004) The presenilin C-terminus is required for ER-retention, nicastrin-binding and gamma-secretase activity. EMBO J 23(24):4738–4748. doi:10.1038/sj.emboj.7600478
65. Kaether C, Scheuermann J, Fassler M, Zilow S, Shirotani K, Valkova C, Novak B, Kacmar S, Steiner H, Haass C (2007) Endoplasmic reticulum retention of the gamma-secretase complex component Pen2 by Rer1. EMBO Rep 8(8):743–748. doi:10.1038/sj.embor.7401027
66. Spasic D, Raemaekers T, Dillen K, Declerck I, Baert V, Serneels L, Fullekrug J, Annaert W (2007) Rer1p competes with APH-1 for binding to nicastrin and regulates gamma-secretase complex assembly in the early secretory pathway. J Cell Biol 176(5):629–640. doi:10.1083/jcb.200609180
67. Bonifacino JS, Cosson P, Shah N, Klausner RD (1991) Role of potentially charged transmembrane residues in targeting proteins for retention and degradation within the endoplasmic reticulum. EMBO J 10(10):2783–2793
68. Berezovska O, Lleo A, Herl LD, Frosch MP, Stern EA, Bacskai BJ, Hyman BT (2005) Familial Alzheimer's disease presenilin 1 mutations cause alterations in the conformation of presenilin and interactions with amyloid precursor protein. J Neurosci 25(11):3009–3017. doi:10.1523/JNEUROSCI. 0364-05.2005
69. Chau DM, Crump CJ, Villa JC, Scheinberg DA, Li YM (2012) Familial Alzheimer disease presenilin-1 mutations alter the active site conformation of gamma-secretase. J Biol Chem 287(21):17288–17296. doi:10.1074/jbc.M111.300483
70. Isoo N, Sato C, Miyashita H, Shinohara M, Takasugi N, Morohashi Y, Tsuji S, Tomita T, Iwatsubo T (2007) Abeta42 overproduction associated with structural changes in the catalytic pore of gamma-secretase: common effects of Pen-2 N-terminal elongation and fenofibrate. J Biol Chem 282(17):12388–12396. doi:10.1074/jbc.M611549200
71. Querfurth HW, Selkoe DJ (1994) Calcium ionophore increases amyloid beta peptide production by cultured cells. Biochemistry 33(15):4550–4561. doi:10.1021/bi00181a016
72. Schultz ML, Tecedor L, Chang M, Davidson BL (2011) Clarifying lysosomal storage diseases. Trends Neurosci 34(8):401–410. doi:10.1016/j.tins.2011.05.006
73. McBrayer M, Nixon RA (2013) Lysosome and calcium dysregulation in Alzheimer's disease: partners in crime. Biochem Soc Trans 41(6):1495–1502. doi:10.1042/BST20130201
74. Zhang X, Garbett K, Veeraraghavalu K, Wilburn B, Gilmore R, Mirnics K, Sisodia SS (2012) A role for presenilins in autophagy revisited: normal acidification of lysosomes in cells lacking PSEN1 and PSEN2. J Neurosci 32(25):8633–8648. doi:10.1523/JNEUROSCI. 0556-12.2012
75. Frykman S, Hur JY, Franberg J, Aoki M, Winblad B, Nahalkova J, Behbahani H, Tjernberg LO (2010) Synaptic and endosomal localization of active gamma-secretase in rat brain. PLoS One 5(1):e8948. doi:10.1371/journal.pone.0008948
76. Siman R, Flood DG, Thinakaran G, Neumar RW (2001) Endoplasmic reticulum stress-induced cysteine protease activation in cortical neurons: effect of an Alzheimer's disease-linked presenilin-1 knock-in mutation. J Biol Chem 276(48):44736–44743. doi:10.1074/jbc.M104092200
77. Liang G, Wang Q, Li Y, Kang B, Eckenhoff MF, Eckenhoff RG, Wei H (2008) A presenilin-1 mutation renders neurons vulnerable to isoflurane toxicity. Anesth Analg 106(2):492–500. doi:10.1213/ane.0b013e3181605b71, table of contents
78. Janicki SM, Stabler SM, Monteiro MJ (2000) Familial Alzheimer's disease presenilin-1 mutants potentiate cell cycle arrest. Neurobiol Aging 21(6):829–836. doi:10.1016/S0197-4580(00)00222-0
79. Janicki SM, Monteiro MJ (1999) Presenilin overexpression arrests cells in the G1 phase of the cell cycle. Arrest potentiated by the Alzheimer's disease PS2(N141I)mutant. Am J Pathol 155(1):135–144. doi:10.1016/S0002-9440(10)65108-5

80. Johnston LA, Edgar BA (1998) Wingless and Notch regulate cell-cycle arrest in the developing Drosophila wing. Nature 394(6688): 82–84. doi:10.1038/27925
81. Athan ES, Williamson J, Ciappa A, Santana V, Romas SN, Lee JH, Rondon H, Lantigua RA, Medrano M, Torres M, Arawaka S, Rogaeva E, Song YQ, Sato C, Kawarai T, Fafel KC, Boss MA, Seltzer WK, Stern Y, St George-Hyslop P, Tycko B, Mayeux R (2001) A founder mutation in presenilin 1 causing early-onset Alzheimer disease in unrelated Caribbean Hispanic families. Jama 286(18):2257–2263. doi: 10.1001/jama.286.18.2257
82. Park HK, Na DL, Lee JH, Kim JW, Ki CS (2008) Identification of PSEN1 and APP gene mutations in Korean patients with early-onset Alzheimer's disease. J Korean Med Sci 23(2):213–217. doi:10.3346/jkms.2008.23.2.213
83. Goldman JS, Reed B, Gearhart R, Kramer JH, Miller BL (2002) Very early-onset familial Alzheimer's disease: a novel presenilin 1 mutation. Int J Geriatr Psychiatry 17(7):649–651. doi:10.1002/gps.657
84. Kim SD, Kim J (2008) Sequence analyses of presenilin mutations linked to familial Alzheimer's disease. Cell Stress Chaperones 13(4): 401–412. doi:10.1007/s12192-008-0046-0